PROCEEDINGS OF SCIENCE

Dark matter study from Lagrangian to data:
in the FeynRules/MadGraph5_aMC@NLO framework

Kentarou Mawatari*
Laboratoire de Physique Subatomique et de Cosmologie, Université Grenoble-Alpes, CNRS/IN2P3, 53 Avenue des Martyrs, F-38026 Grenoble, France
Theoretische Natuurkunde and IIHE/ELEM, Vrije Universiteit Brussel, and International Solvay Institutes, Pleinlaan 2, B-1050 Brussels, Belgium
E-mail: kentarou.mawatari@lpsc.in2p3.fr

We present recent development of simulation tools to study dark matter at colliders as well as for astrophysical and cosmological observables in the FeynRules/MadGraph5_aMC@NLO framework. We show some results for simplified dark matter models with *s*-channel spin-1 mediators as an example.

11th International Workshop Dark Side of the Universe 2015
14-18 December 2015
Yukawa Institute for Theoretical Physics, Kyoto University Japan

*Speaker.

PoS(DSU2015)054

1. Introduction

Various cosmological and astrophysical observations provide strong hints for the existence of the dark side of the Universe, e.g. dark matter (DM). DM cannot be described in the standard model (SM) of particle physics and so far very little is known about the nature of DM. Therefore, in order to detect it and measure its properties, various types of DM searches have been in progress;

- Direct detection: underground nuclear recoil experiments aimed at detecting galactic DM scattering off atomic nuclei;
- Indirect detection: searches for DM annihilation in the galaxy or nearby dense sources via measurements of, e.g. gamma-rays and neutrinos;
- Collider experiments: searches in channels with large missing transverse energy (MET).

For broad and systematic DM searches at the LHC, the LHC Dark Matter Working Group (LHC DM WG) [1] was formed recently, based on the previous ATLAS-CMS Dark Matter Forum [2], and proposed the simplified DM model framework for early LHC Run-2. One of the benchmark models is a model with s-channel mediators, where DM is assumed to be a single massive particle which interacts with the SM particles via an s-channel new boson.

Following the above recommendation, we recently illustrated the feasibility of having a fully general implementation of s-channel simplified DM models in the FEYNRULES [3, 4]/MADGRAPH5_AMC@NLO [5] (MG5AMC henceforth) framework [6], together with articles focusing on the loop-induced processes [7] and the mono-Z final state [8]. We showed how predictions and event generation both for the spin-0 and spin-1 mediator scenarios can be achieved at next-to-leading order (NLO) QCD accuracy in a fully automatic way for a wide set of observable/final states. In this proceedings we briefly report the spin-1 mediator case, while one can find the more details and the spin-0 case in [6]. A comprehensive study for the spin-0 mediator was also presented recently in [9].

2. Simplified dark matter models with s-channel spin-1 mediators

In the framework of s-channel simplified models, the interaction Lagrangian of a spin-1 mediator (Y_1) with a Dirac fermion DM (X) is given by

$$\mathscr{L}_X^{Y_1} = \bar{X}\gamma_\mu(g_X^V + g_X^A\gamma_5)X\,Y_1^\mu\,, \tag{2.1}$$

and with quarks by

$$\mathscr{L}_{\rm SM}^{Y_1} = \sum_{i,j}\Big[\bar{d}_i\gamma_\mu(g^V_{d_{ij}} + g^A_{d_{ij}}\gamma_5)d_j + \bar{u}_i\gamma_\mu(g^V_{u_{ij}} + g^A_{u_{ij}}\gamma_5)u_j\Big]Y_1^\mu\,, \tag{2.2}$$

where d and u denote down- and up-type quarks, respectively, (i, j=1,2,3) are flavour indices, and $g^{V/A}$ are the vector/axial-vector couplings of DM and quarks. Note that we adopt this notation according to the actual implementation in FEYNRULES. The model file, dubbed as DMSIMP, including an alternative choice for the spin of DM particle (complex scalar), can be downloaded at the FEYNRULES repository [10].

The pure vector and pure axial-vector mediator scenarios are given by setting the parameters in the Lagrangians (2.1) and (2.2) to

$$g^V_X \equiv g_X \quad \text{and} \quad g^A_X = 0 \tag{2.3}$$

$$g^V_{u_{ii}} = g^V_{d_{ii}} \equiv g_{\rm SM} \quad \text{and} \quad g^A_{u_{ii}} = g^A_{d_{ii}} = 0 \tag{2.4}$$

and

$$g^V_X = 0 \quad \text{and} \quad g^A_X \equiv g_X \tag{2.5}$$

$$g^V_{u_{ii}} = g^V_{d_{ii}} = 0 \quad \text{and} \quad g^A_{u_{ii}} = g^A_{d_{ii}} \equiv g_{\rm SM}\,, \tag{2.6}$$

respectively, where we assume quark couplings to the mediator to be flavour universal and set all flavour off-diagonal couplings to zero. With this simplification of a single universal coupling for the SM–Y_1 interactions, the model has only four independent parameters, *i.e.* two couplings and two masses:

$$\{g_X, g_{\rm SM}, m_X, m_Y\}\,. \tag{2.7}$$

We note that the mediator width is calculated from the above parameters, and automatically computed by using the MadWidth module [11] in our framework.

Finding a signal of DM in this parameter space (or to constrain these parameters) is the primary goal of the DM searches at the LHC Run-2 [2], and the most important signature in this model is a jet plus MET. The di-jet final state via the Y_1 Drell–Yan process can be an important complementary channel, i.e. resonance searches without MET.

3. Dark matter production with jets

In this section, we present the impact of the NLO-QCD corrections on DM pair production with jets, *i.e.*,

$$pp \to X\bar{X} + j(j)\,. \tag{3.1}$$

In MG5aMC the code and events for the above process can be automatically generated by issuing the following commands:

```
./bin/mg5_aMC
> import model DMsimp_s_spin1
> generate p p > xd xd~ j [QCD]
> add process p p > xd xd~ j j [QCD]
> output
> launch
```

We have checked that our model can reproduce the SM predictions for $pp \to Zj(j) \to \tau^+\tau^- j(j)$ by adjusting the corresponding coupling and mass parameters.

To illustrate the effect of the higher-order corrections, we consider pure vector, Eqs. (2.3) and (2.4), or pure axial-vector, Eqs. (2.5) and (2.6), couplings with a simplified flavour structure. We take

$$(g_X, g_{\rm SM}) = (1, 0.25) \tag{3.2}$$

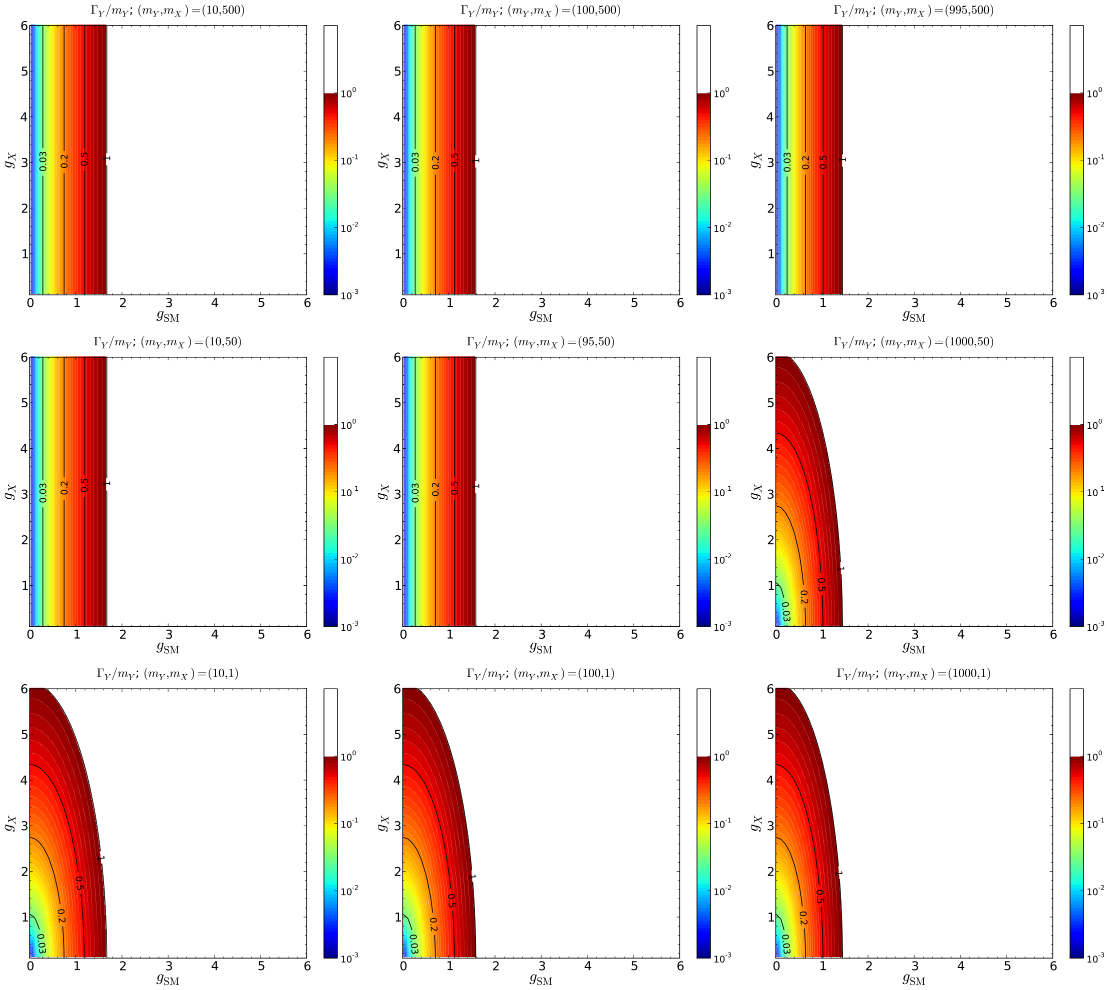

Figure 1: Ratio of the mediator width to its mass in the $g_{\rm SM}$–g_X plane for different mass choices.

as our benchmark for the spin-1 mediator scenario. This benchmark leads to $\Gamma_Y/m_Y \sim 0.05$ for $m_Y > 2m_X$ and $\Gamma_Y/m_Y \sim 0.025$ for $m_Y < 2m_X$, both for the vector and axial-vector cases; see also Fig. 1.

In Table 1 we present LO and NLO cross sections for $pp \to X\bar{X} + j$ at the center-of-mass energy $\sqrt{s} = 13$ TeV. The central value μ_0 for the renormalisation (μ_R) and factorisation (μ_F) scales is set to $H_T/2$, where H_T is the sum of the transverse momenta of all jets in the event and the missing transverse energy. The scale uncertainty is estimated by varying the scales μ_R and μ_F, independently, by a factor two around μ_0. We adopt the five-flavour scheme and the LO and NLO NNPDF2.3 set [12]. A graphical summary of the results is also shown in Fig. 2.

The production rate strongly depends on the both masses as well as on the kinematic cuts, and varies by orders of magnitude in the parameter scan. On the other hand, the K factors, *i.e.* higher-order effects, are not so sensitive to the mass spectra. As expected, most of the results at NLO accuracy display significantly smaller scale uncertainties compared to the LO calculations.

Figure 3 shows the MET distributions at LO and NLO for four benchmark points of the simplified model. The NLO effects in the distributions do not depend on the mass relation between the

(m_Y, m_X) [GeV]			vector MET > 150 GeV	vector MET > 300 GeV
100	undecayed	$\sigma_{\rm LO}$ [pb]	$2.148\times10^{2}\,^{+10.6}_{-9.3}\,\pm1.5\,\%$	$1.616\times10^{1}\,^{+14.4}_{-12.0}\,\pm1.0\,\%$
		$\sigma_{\rm NLO}$ [pb]	$3.011\times10^{2}\,^{+6.6}_{-5.9}\,\pm0.5\,\%$	$2.121\times10^{1}\,^{+7.3}_{-7.1}\,\pm0.6\,\%$
		K factor	1.40	1.31
(100, 1)	$m_Y > 2m_X$	$\sigma_{\rm LO}$ [pb]	$1.100\times10^{2}\,^{+10.6}_{-9.3}\,\pm1.5\,\%$	$0.822\times10^{1}\,^{+14.4}_{-12.0}\,\pm1.1\,\%$
		$\sigma_{\rm NLO}$ [pb]	$1.530\times10^{2}\,^{+6.5}_{-5.7}\,\pm0.5\,\%$	$1.100\times10^{1}\,^{+7.4}_{-7.2}\,\pm0.6\,\%$
		K factor	1.39	1.34
(95, 50)	$m_Y \lesssim 2m_X$	$\sigma_{\rm LO}$ [pb]	$1.117\times10^{1}\,^{+11.0}_{-9.6}\,\pm1.5\,\%$	$0.988\times10^{0}\,^{+14.7}_{-12.2}\,\pm1.1\,\%$
		$\sigma_{\rm NLO}$ [pb]	$1.512\times10^{1}\,^{+6.0}_{-5.5}\,\pm0.5\,\%$	$1.281\times10^{0}\,^{+6.8}_{-6.8}\,\pm0.6\,\%$
		K factor	1.35	1.30
(100, 500)	$m_Y < 2m_X$	$\sigma_{\rm LO}$ [pb]	$7.043\times10^{-3}\,^{+17.4}_{-14.0}\,\pm4.3\,\%$	$2.329\times10^{-3}\,^{+18.9}_{-15.0}\,\pm4.6\,\%$
		$\sigma_{\rm NLO}$ [pb]	$7.804\times10^{-3}\,^{+5.3}_{-6.4}\,\pm2.2\,\%$	$2.411\times10^{-3}\,^{+5.5}_{-6.8}\,\pm2.3\,\%$
		K factor	1.11	1.04
(m_Y, m_X) [GeV]			axial-vector MET > 150 GeV	axial-vector MET > 300 GeV
100	undecayed	$\sigma_{\rm LO}$ [pb]	$2.130\times10^{2}\,^{+10.6}_{-9.3}\,\pm1.6\,\%$	$1.573\times10^{1}\,^{+14.4}_{-12.0}\,\pm1.1\,\%$
		$\sigma_{\rm NLO}$ [pb]	$3.063\times10^{2}\,^{+6.9}_{-6.1}\,\pm0.5\,\%$	$2.153\times10^{1}\,^{+7.7}_{-7.4}\,\pm0.6\,\%$
		K factor	1.44	1.37
(100, 1)	$m_Y > 2m_X$	$\sigma_{\rm LO}$ [pb]	$1.101\times10^{2}\,^{+10.6}_{-9.3}\,\pm1.6\,\%$	$0.825\times10^{1}\,^{+14.4}_{-12.1}\,\pm1.1\,\%$
		$\sigma_{\rm NLO}$ [pb]	$1.549\times10^{2}\,^{+6.8}_{-6.0}\,\pm0.5\,\%$	$1.127\times10^{1}\,^{+7.4}_{-7.2}\,\pm0.6\,\%$
		K factor	1.41	1.37
(95, 50)	$m_Y \lesssim 2m_X$	$\sigma_{\rm LO}$ [pb]	$3.070\times10^{0}\,^{+11.6}_{-10.0}\,\pm1.5\,\%$	$3.359\times10^{-1}\,^{+14.9}_{-12.4}\,\pm1.2\,\%$
		$\sigma_{\rm NLO}$ [pb]	$4.093\times10^{0}\,^{+6.0}_{-5.7}\,\pm0.5\,\%$	$4.302\times10^{-1}\,^{+6.7}_{-6.9}\,\pm0.7\,\%$
		K factor	1.33	1.28
(100, 500)	$m_Y < 2m_X$	$\sigma_{\rm LO}$ [pb]	$2.298\times10^{-3}\,^{+18.1}_{-14.5}\,\pm5\,\%$	$7.839\times10^{-4}\,^{+19.5}_{-15.4}\,\pm5.3\,\%$
		$\sigma_{\rm NLO}$ [pb]	$2.502\times10^{-3}\,^{+5.9}_{-6.8}\,\pm2.5\,\%$	$7.972\times10^{-4}\,^{+6.2}_{-7.3}\,\pm2.6\,\%$
		K factor	1.09	1.02

Table 1: LO and NLO cross sections and corresponding K factors for DM pair production in association with a jet for the vector (top) and axial-vector (bottom) mediator scenario at the 13-TeV LHC, where 150 and 300 GeV MET cuts are imposed. The uncertainties represent the scale and PDF uncertainties in per cent, respectively. We show several benchmark model points for the mediator and DM masses with the coupling parameters $(g_X, g_{\rm SM}) = (1, 0.25)$.

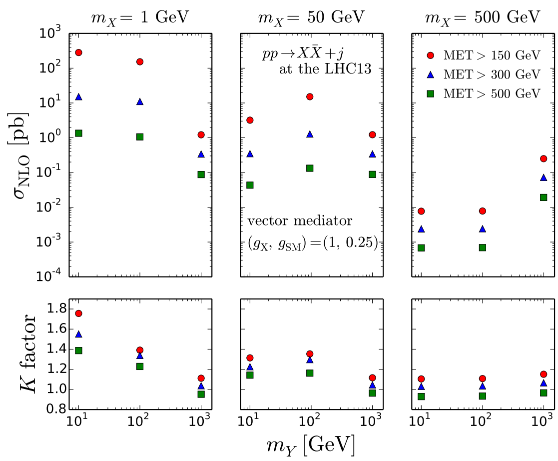

Figure 2: Summary plot of NLO cross sections and corresponding K factors.

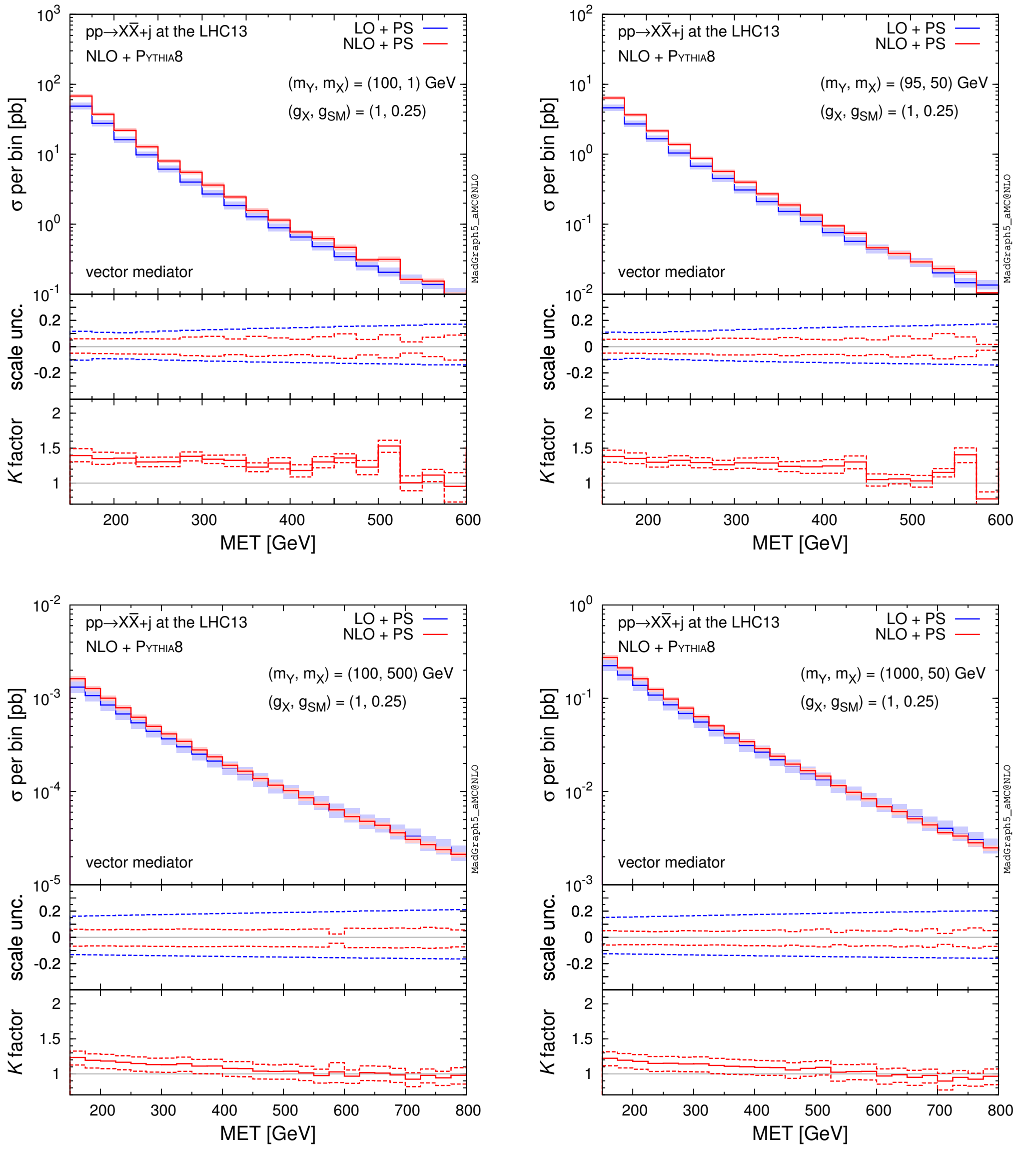

Figure 3: MET distributions for $pp \to X\bar{X} + j$ at the 13-TeV LHC for four benchmark points specified by (m_Y, m_X), where we assume a pure vector mediator and Dirac DM. The middle and bottom panels show the differential scale uncertainties and K factors, respectively.

mediator and the DM, *i.e.* on-shell or off-shell, but do depend on the energy scale of the final state. The NLO corrections are different for different MET regions, with the largest NLO corrections occurring in the lower MET regions where the rate is the highest. Hence the careful estimation of NLO effects is very important for accurate LHC studies of DM in each signal region.

4. Astrophysical observables

Not only collider searches but also astrophysical and cosmological observables should be taken into account for having viable DM models, such as relic density and direct/indirect detection constraints. MadDM has recently been developed in the FeynRules/MG5aMC framework to

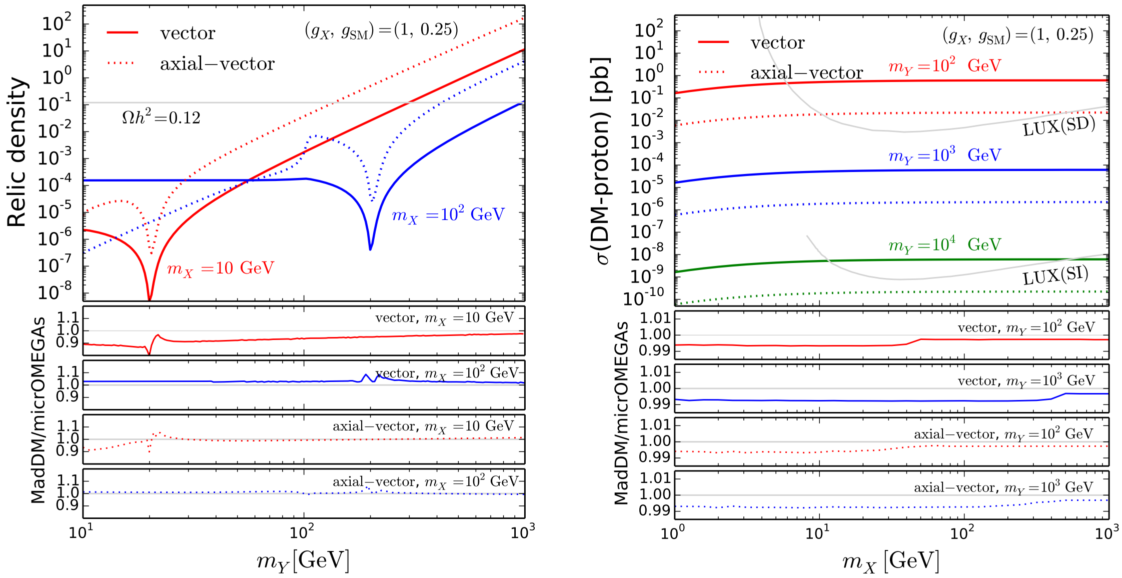

Figure 4: Left: DM relic density as a function of the mediator mass. Right: DM–proton elastic scattering cross section as a function of the DM mass. A simplified DM model with s-channel (axial-)vector mediators is considered with the coupling parameters $(g_X, g_{SM}) = (1, 0.25)$. In the bottom panels comparisons between MADDM and MICROMEGAS are shown.

compute DM relic abundance [13] and to perform calculations relevant to the direct detection of DM [14]. After downloading the MADDM folder inside the main MG5AMC, one can run the code as below:[1]

```
./maddm.py
> Enter model name: DMsimp_s_spin1_LO
> Enter project name (DMsimp_s_spin1_LO):
> Calculate relic density? [y] (y/n)
> Calculate direct detection cross sections? [y] (y/n)
> Simulate DM scattering events off nuclei? [y] (y/n)
> Enter DM candidate: ~xd
```

As an illustration, Fig. 4 shows numerical results of the relic density and the DM–proton elastic scattering cross section for s-channel simplified models. We find good agreement with the results from MICROMEGAS [15, 16].

Acknowledgments

KM wishes to thank M. Backović, M. Krämer, F. Malotni, A. Martini and M. Pellen for the collaboration, and also F. Hosseini, J.D. Silva and K. Yamashita for the MADDM and MICROMEGAS comparison. The participation in the DSU workshop was supported by the Theory-LHC-France initiative of the CNRS (INP/IN2P3).

[1]Different from the `DMsimp_s_spin1` model, `DMsimp_s_spin1_LO` keeps all the quark masses for the direct detection calculation and can only compute tree-level amplitudes [10].

References

[1] http://lpcc.web.cern.ch/LPCC/index.php?page=dm_wg.

[2] D. Abercrombie et al., *Dark Matter Benchmark Models for Early LHC Run-2 Searches: Report of the ATLAS/CMS Dark Matter Forum*, 1507.00966.

[3] A. Alloul, N. D. Christensen, C. Degrande, C. Duhr and B. Fuks, *FeynRules 2.0 - A complete toolbox for tree-level phenomenology*, Comput. Phys. Commun. **185** (2014) 2250–2300, [1310.1921].

[4] C. Degrande, *Automatic evaluation of UV and R2 terms for beyond the Standard Model Lagrangians: a proof-of-principle*, Comput. Phys. Commun. **197** (2015) 239–262, [1406.3030].

[5] J. Alwall, R. Frederix, S. Frixione, V. Hirschi, F. Maltoni, O. Mattelaer et al., *The automated computation of tree-level and next-to-leading order differential cross sections, and their matching to parton shower simulations*, JHEP **07** (2014) 079, [1405.0301].

[6] M. Backovic, M. Kramer, F. Maltoni, A. Martini, K. Mawatari and M. Pellen, *Higher-order QCD predictions for dark matter production at the LHC in simplified models with s-channel mediators*, Eur. Phys. J. **C75** (2015) 482, [1508.05327].

[7] O. Mattelaer and E. Vryonidou, *Dark matter production through loop-induced processes at the LHC: the s-channel mediator case*, Eur. Phys. J. **C75** (2015) 436, [1508.00564].

[8] M. Neubert, J. Wang and C. Zhang, *Higher-Order QCD Predictions for Dark Matter Production in Mono-Z Searches at the LHC*, JHEP **02** (2016) 082, [1509.05785].

[9] C. Arina, M. Backović, E. Conte, B. Fuks, J. Guo, J. Heisig, B. Hespel, M. Krámer, F. Maltoni, A. Martini, K. Mawatari, M. Pellen and E. Vryonidou, *A comprehensive approach to dark matter studies: exploration of simplified top-philic models*, 1605.09242.

[10] http://feynrules.irmp.ucl.ac.be/wiki/DMsimp.

[11] J. Alwall, C. Duhr, B. Fuks, O. Mattelaer, D. G. Ozturk and C.-H. Shen, *Computing decay rates for new physics theories with FeynRules and MadGraph 5_aMC@NLO*, Comput. Phys. Commun. **197** (2015) 312–323, [1402.1178].

[12] R. D. Ball et al., *Parton distributions with LHC data*, Nucl. Phys. **B867** (2013) 244–289, [1207.1303].

[13] M. Backovic, K. Kong and M. McCaskey, *MadDM v.1.0: Computation of Dark Matter Relic Abundance Using MadGraph5*, Physics of the Dark Universe **5-6** (2014) 18–28, [1308.4955].

[14] M. Backovic, A. Martini, O. Mattelaer, K. Kong and G. Mohlabeng, *Direct Detection of Dark Matter with MadDM v.2.0*, Phys. Dark Univ. **9-10** (2015) 37–50, [1505.04190].

[15] G. Belanger, F. Boudjema, A. Pukhov and A. Semenov, *MicrOMEGAs 2.0: A Program to calculate the relic density of dark matter in a generic model*, Comput. Phys. Commun. **176** (2007) 367–382, [hep-ph/0607059].

[16] G. Belanger, F. Boudjema, A. Pukhov and A. Semenov, *Dark matter direct detection rate in a generic model with micrOMEGAs 2.2*, Comput. Phys. Commun. **180** (2009) 747–767, [0803.2360].